



ELSEVIER

Contents lists available at [ScienceDirect](#)

Ad Hoc Networks

journal homepage: www.elsevier.com/locate/adhoc

Cross-layer analysis via Markov models of incremental redundancy hybrid ARQ over underwater acoustic channels [☆]

Beatrice Tomasi ^a, Paolo Casari ^b, Leonardo Badia ^{b,*}, Michele Zorzi ^b

^a Woods Hole Oceanographic Institution, Woods Hole, MA, United States

^b Department of Information Engineering, University of Padova, Padova, Italy

ARTICLE INFO

Article history:

Received 28 February 2014

Received in revised form 12 July 2014

Accepted 29 July 2014

Available online xxx

Keywords:

Cross-layer design and optimization

Performance evaluation

Data-link layer

Error correction

Underwater communications

ABSTRACT

Underwater acoustic networks make it possible to wirelessly convey information, e.g., coming from measurements and sensing applications from under water to the surface. However, underwater communications are characterized by long delays, small available bandwidths and high error rates. These aspects may significantly affect the design of a reliable data-link layer for such systems. In this paper, we assess the performance of hybrid automatic repeat request error control schemes and we evaluate their application to improve the reliability of time-varying underwater acoustic links. We employ a parametric Markov model, which has been trained over channel traces collected during at-sea experiments. The results, based on both experimental data and analysis, suggest that parametric probabilistic representations, such as the considered Markov model, are good candidates for describing the correlated underwater acoustic channel dynamics, and may be employed to achieve a realistic evaluation of the data-link layer performance for underwater acoustic scenarios. Analytical and simulation results confirm that incremental redundancy improves the throughput of underwater acoustic links, even when real channel conditions, such as those encountered in the considered experiments, have wide dynamics over time. Finally, this kind of evaluations, beyond the data-link design, can also be employed at the network level for routing and network deployment considerations.

© 2014 Published by Elsevier B.V.

1. Introduction

Underwater acoustic (UWA) communications and networks have recently received considerable attention from the research community, since they make it possible to wirelessly convey information from under water to the

surface, thus enabling several ocean-related applications, in particular for sensing and monitoring of seismic activity, oil leakages, chemical pollutions, and so on [2]. However, the harsh underwater acoustic channel conditions give rise to several challenges related to reliability, latency, and energy consumption [3]. In particular, the data-link design is challenging since data rates of underwater acoustic transmissions can reach tens of kilobits per second at most (over typical distances of the order of kilometers) [4]. Moreover, error control can be critical since, in such a scenario, employing forward error correction (FEC) would require a conservative dimensioning of the amount of redundancy required for error correction, while Automatic Repeat reQuest (ARQ) can lead to longer delays, since the sound propagates underwater with a speed of

[☆] A preliminary work [1] comprising part of this paper has been presented at ACM WUWNet, 2010. This work was supported in part by the NATO Undersea Research Center, La Spezia, Italy, under contracts no. 40800700 (ref. NURC-010-08) and 40900654, and the Italian Institute of Technology (IIT), Genova, Italy, within the project SEED framework (NAUTILUS project).

* Corresponding author.

E-mail address: badia@dei.unipd.it (L. Badia).

approximately 1500 m/s: thus, round trip times can be of the order of a few seconds, even if a very small packet size is employed.

We propose and evaluate the use of hybrid ARQ (HARQ) schemes, where data packets are protected with FEC, but retransmissions are allowed when required. In this way, the codeword redundancy can be adaptively tuned by retransmissions as needed. For this very same reason, HARQ schemes have been originally proposed to address unreliability in terrestrial radio time-varying channels, e.g., for mobile wireless networks. However, UWA communications are even more sensitive to the physical layer, and therefore the data-link design requires a careful cross-layer assessment. Indeed, UWA communications may suffer from heavy fluctuations of the channel quality, similar to the wireless channel, as shown in [5,6]. HARQ is therefore a good candidate for error control, also because it requires, as a feedback control message, a simple acknowledgment from the receiver instead of more detailed channel state information, which may become outdated given the long propagation delays under water.

To the best of our knowledge, a cross-layer performance evaluation of HARQ techniques for UWA communications is a missing contribution in the literature. This can be justified by the lack of an accepted statistical channel or packet error model for UWA communications, which is still an open problem [7–9]. To overcome this hurdle, we propose to employ a Markov statistical model, able to represent time correlation of the channel states. Markov models are recognized as both valid and useful means to represent terrestrial radio channels and to analytically characterize techniques such as ARQ/HARQ [10]. A similar contribution for the UWA scenario does not exist, and therefore, we here present an analytical framework to derive the performance of HARQ schemes in UWA communications.

More specifically, we evaluate the data-link layer performance through the following steps: (i) estimation of the channel statistics and derivation of the Signal-to-Noise Ratio (SNR); (ii) derivation of the corresponding reliability regions of the HARQ scheme for capacity-achieving codes, as described in [11,12]; (iii) quantization of the channel quality through the method proposed in [13], in order to obtain a Finite State Markov Chain (FSMC); and (iv) overall performance evaluation, considering different HARQ schemes.

To validate this general framework also in the UWA scenario, we focus on a specific case study, consisting of channel qualities measured during at-sea experiments. In this scenario, we test the Markov assumption and we apply the characterization via an FSMC, which enables the derivation of various performance metrics. Also, note that the scenario considers just two nodes, and therefore interference is absent. However, it would be possible to incorporate interference as well by considering the statistics of a Signal-to-Interference-plus-Noise Ratio (SINR) as opposed to the plain SNR. The obtained results can be generalized to scenarios with channel dynamics similar to those observed in the considered case. In addition, the proposed methodology can be applied to any other experimental SNR trace, and is therefore of significant practical value.

The remainder of this paper is organized as follows. Section 2 gives the background for the present study in terms of related work and possible cases of application. In Section 3, we describe the mathematical representation of the HARQ technique, the experimental SNR traces and the quantization of the channel state. Then, in Section 4, we combine these parts to derive the Markov model for HARQ with or without Incremental Redundancy (IR), used to evaluate the performance in terms of throughput, number of retransmissions per correctly received packet, and probability of frame discarding. Section 5 presents the numerical results and validation of the proposed framework by considering all the critical points. Finally, Section 6 concludes the paper.

2. Related work and applications scenarios

Underwater networks are strongly affected by long propagation delays, high error probabilities and low data rates [4,14]. Thus, most of the studies focus on simplified mechanisms for error control, and it is often claimed that half duplexing constraints limit the choice of ARQ mechanisms to the simple Stop-and-Wait implementation. Alternatively, just FEC is employed. We argue that in reality the best choice for such a critical scenario would be to set for a hybrid ARQ, where channel impairments are mitigated by error correction coding, but at the same time ARQ allows a better control of momentary channel fades by retransmitting packets on-demand.

Moreover, a number of solutions can be adopted at the transmission level, to circumvent the constraint posed by the half-duplex channel. In [15] it is argued that, by properly estimating the propagation time, which is actually well predictable in stationary conditions, transmissions and exchange of acknowledgments can be coordinated so as to avoid mutual collisions between the transmitter and the receiver. A similar idea is exploited in [16], where a proper duty cycle is set on the activities of both nodes, which results in an improved SW mechanism where exchange of packets is almost continuous.

When looking at the most common applications of underwater networks [3], it is also worthwhile remarking that in many scenarios the generation rate of the source data is considerably low: this is the case of marine monitoring for seismic activity or assisted navigation. This means that one can often assume, as we do in this paper, that the ARQ reduces to an *ideal* ARQ scenario where a limited number of pending packets (just one) is considered, thus Selective Repeat or Stop-and-Wait ARQ coincide [13]. It is actually an extreme case of a low Bandwidth-Delay-Product scenario, motivated by the fact that we have both undesirable properties of high propagation delay but also extremely limited bandwidth [5].

ARQ over channels with high propagation delays can also be handled using expedients such as the one proposed in [17], where idle times of the channels can be exploited to improve the retransmission mechanism, by adding a second replica of retransmitted packets. Similarly, ARQ can benefit from and also improve the network performance in multi-hop contexts, and it is better if

implemented on a per-hop basis [18]. Cooperative and opportunistic paradigms can also be employed to this end [19]. While such ideas are not directly exploited in the present paper, they would be actually easy to integrate with the overall framework.

Finally, the work is based on the analysis developed in [20] to study the HARQ process based on an efficient channel representation by means of a Markov chain. The key idea is to pursue the characterization of the channel directly aiming at the HARQ status, thus considering Markov states that are related to the HARQ process. However, that contribution is entirely different since it refers to analytical models for a wireless radio transmission, a scenario that is much better understood than underwater acoustic communications. One of the main goals of this paper is to demonstrate the generality and practicality of the model, by looking at an entirely different scenario and channel traces taken from real measurements.

In this sense, a preliminary version of this paper appeared in [1], where the focus was however limited to showing the performance evaluation for hybrid ARQ on underwater channels thanks to the proposed model. With respect to that contribution, this paper brings considerable additions in validating the applicability of the model itself rather than just discussing its capabilities. In particular, we consider a correlated channel and present a detailed discussion on whether the quantization of the channel state should take into account the correlation of the channel evolution, which causes a distortion of the reliable region. Additionally, we discuss the update frequency of model training, which is shown to be reasonable for practical implementations. Finally, we relax the assumption of *ideal* ARQ, which enables us to generalize the conclusions found by the proposed framework. None of these aspects is considered in [1].

For what concerns practical applications, our approach can be used as a general evaluation instrument, where communication metrics are extracted from physical parameters of the network. Apart from practical evaluations on real testbeds [4], which would be time- and resource-consuming, the only alternative to such an approach would be to evaluate the performance from the measured traces, which can be done only offline. Instead, our methodology can be applied to real-time applications, since performance metrics can be evaluated even before knowing the full channel evolution, as long as a sufficiently reliable estimate of the channel statistics is available. The model does rely on a Markov approach, yet the time to train the model does not need to be very long, and the statistics can be dynamically updated.

The assessment of this underwater scenario can be integrated with other technical parameters of the transmission devices to obtain a flexible framework for data-link design (specifically, to test the coding protection to include in the HARQ) for underwater networks. In practice, if several candidate coding schemes are available to be applied to the transmission of at-sea measurements collected by underwater sensors, one can immediately verify how they perform in terms of reliability, delay, and throughput, and decide for the most suitable one. It can be thought of as a practical real-time implementation on real underwater

modems, to adapt the coding protection (chosen among a limited number of alternatives) based on quality requirements [4,21].

Finally, we remark that our model is entirely analytical. The proposed Markov chain can be combined with other models of the upper layers (network, transport, application), so as to investigate a cross-layer optimization of transmission parameters, possibly involving networking analysis for route selection and diversity, or the development of flow control techniques.

3. Transmission system model

The characterization of a data-link layer for underwater communication must take into account physical layer aspects, and is therefore an inherently cross-layer design problem. Thus, we consider a threefold mathematical characterization of the system under investigation. First, we describe the model of HARQ, based on standard channel coding performance models [11,12]. Second, we describe the underwater physical layer as a Markov channel whose statistics are derived from the experimental campaign. Finally, we discuss how a low-complexity FSMC formulation that leads to a simple model based on quantized channel states can be derived to evaluate the HARQ performance.

3.1. HARQ model

The name “hybrid ARQ” implies that automatic retransmission request is used together with forward error correction. HARQ can be represented as the transmission of multiple *information frames*, which are encoded by a low-rate code. The resulting codeword is divided into multiple fragments that are transmitted as HARQ packets. For simplicity, we assume that all fragments have the same size, and any of them alone is sufficient to recover the whole codeword, and thus the frame, in good channel conditions.

The receiver replies to the packets arriving from the transmitter with either an acknowledgment (ACK) or negative acknowledgment (NACK), indicating correct or incorrect reception, respectively. As per classic ARQ, a NACK triggers a retransmission of the erroneously received packet. Still, this retransmission and the associated decoding at the receiver side can take place in two manners, which are usually referred to as Type I and Type II HARQ [22]. In Type I HARQ, a transmission and all subsequent retransmissions are managed at the receiver without any combination of the contents of different fragments, so that the decoding process restarts anew each time. This can happen because, e.g., “retransmission” literally means that the same actual packet is sent again (thus, just one fragment of the long codeword is used) or the receiver discards faulty packets without combining them. In Type II HARQ, subsequent detection attempts combine all the received fragments, so as to form a longer codeword with lower rate. Therefore, this scheme is also called Incremental Redundancy (IR) HARQ.

To effectively model the successful reception of a frame, we assume that the decoding performance can be represented in terms of reliability regions [11,12]. Such

assumption holds if the codeword is sufficiently long. Note that reliability regions can be derived for any code and therefore our analysis can be generalized. While the problem of defining the reliability regions for general turbo or Low Density Parity Check (LDPC) codes is out of the scope of this paper, we make use of the results in [11], where the reliability regions are derived in closed-form for “good” LDPC code ensembles.

The authors of [12] describe the performance of the considered codes in terms of SNR thresholds, by taking an information-theoretic point of view. In particular, to determine whether or not a packet is successful, in case the decoder exploits only a single transmitted packet, it is sufficient to verify whether or not the SNR value is above a single threshold ϑ . In Type I HARQ, this same condition is checked at every retransmission. Instead, in IR-HARQ, if $k > 1$ packets are combined, each bearing its own SNR value s_1, \dots, s_k , a *reliability region* of SNRs [11,12] can be determined. A reliability region is the set $\mathcal{R}(k) \subseteq \mathbb{R}^k$ containing the SNR k -tuples for which the decoding failure probability asymptotically vanishes as the codeword length increases. Regardless of the specific shape of the reliability region, if $s > \vartheta$, any k -tuple containing s belongs to the reliability region, as a single transmission with SNR equal to s determines a correct packet reception. However, since the receiver exploits the combination of redundancy from multiple transmissions, a reliability region contains in general also k -tuples where all the elements are lower than ϑ . Finally, if a k -tuple of SNR values $(s_1, \dots, s_k) \in \mathcal{R}(k)$, then the k -tuple $(s_1, \dots, s'_k) \in \mathcal{R}(k)$ as well, for every $s'_k > s_k$ [12]. This directly follows from the fact that if the k th fragment suffices to enable correct decoding if combined with the previous $k - 1$ ones, the reception of the k th fragment with a better SNR would also lead to correct decoding. A representation of the reliability region is therefore enabled by means of a threshold model, where the lowest SNR that the k th transmission should have to ensure successful decoding depends on the sequence $\mathbf{s}^{(k-1)}$ of all previous $k - 1$ SNRs. Such a threshold takes the form

$$\vartheta(\mathbf{s}^{(k-1)}) = \inf\{s_k : (s_1, \dots, s_{k-1}, s_k) \in \mathcal{R}(k)\}, \quad (1)$$

which can be used to verify whether correct decoding occurred at the k th transmission, by checking if $s_k \geq \vartheta(\mathbf{s}^{(k-1)})$. As no packet combining is possible at the first transmission attempt, we have $\vartheta(\mathbf{s}^{(0)}) = \vartheta$, i.e., the SNR is checked against the single-transmission threshold ϑ .

3.2. Experimental SNR traces

To determine if a series of HARQ packets is successfully decoded, it is sufficient to verify if the k -tuple of their SNR values belongs to the reliability region. As a consequence, the packet error process depends on the channel statistics between the source and the receiver.

To apply this reasoning to realistic measurements, we apply the Markov framework for HARQ to measures of the channel quality collected during the sea trial called SubNet09, conducted off the coast of Pianosa island (Italy)

[9]. The used SNR values are estimated from a probing signal (either a hyperbolic frequency modulated sine wave or a sequence of 30 symbols taken from a predefined frequency-hopping pattern). The testbed used during SubNet09 consisted of one vertical array (VA) of hydrophones at different depths (of which we consider H1, H2 and H4, respectively located at a depth of 20, 40, and 80 m), and three Teledyne-Low Frequency acoustic modems [21], each placed on the sea floor at different depths (60–80 m) and distances from the VA. The three transmitters are labeled T1 (1500 m from the VA, depth 60 m), T2 (2200 m from the VA, depth 70 m) and T3 (700 m from the VA, depth 80 m).

Using this deployment, many experiments were conducted, lasting up to ten hours and involving several thousand transmissions, at different times of the day and in different days throughout the summer season. We present here the results for a representative set of traces collected on June 5, 2009. During this experiment, signals were transmitted once every 15 s for 9 h over a downward-refractive medium, and for each signal the SNR was estimated. Although we focus on those measurements, we remark that the same methodology and processing have been applied to other periods, obtaining similar results.

From the collected signals, we can estimate the SNR by considering the entire multipath structure in the channel impulse response, as measured by a non-coherent receiver with a sufficiently long symbol time. From the data set in [9], several SNR time series can be derived. An example is shown in Fig. 1, depicting the time evolution of the SNR over the links from all transmitters to hydrophone H2, which is placed 40 m below the surface. A moving average of the time series taken over 25 samples is also shown as a solid black line.

The figure shows the fluctuations affecting the input SNR at H2 from the three sources. Link T3–H2 (T3 is the closest to H2) experiences the highest and most stable SNR. We also observe that, during the first three hours, link

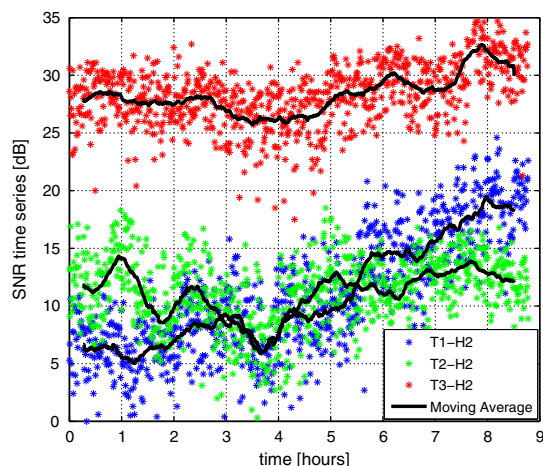


Fig. 1. Measured time series of the SNR over the links from all transmitters to hydrophone H2. A moving average taken over a window of 25 samples is superimposed to the SNR time series as a solid black line.

T2–H2 shows higher SNR than T1–H2, even though T2 is 700 m farther from the receiver than T1. In the following hour they show similar SNRs and eventually T1–H2 has higher SNRs than T2–H2. The moving average of the SNR fluctuates from 7 dB to 19 dB for T1–H2, and from 6 dB to 14 dB for T2–H2. These fluctuations are caused by the environmental phenomena affecting the acoustic propagation, such as temperature and surface conditions, thus giving rise to time variations. The average SNR level is quite high over the T3–H2 link, as the dominating effects are the short distance and a strong line of sight component. A different behavior is observed over T1–H2 and T2–H2 links, i.e., the intermediate and longest distance links respectively, for which the strongest arrivals are affected by multiple reflections on the time-varying surface and on the sea bottom.

To derive our model, we need to estimate the statistics of the SNR; in particular, as will be discussed later, the one-step transition probabilities of the SNR are required. We compute them from time averages over the whole trace (or possibly a portion of it), which implicitly means that the SNR is assumed to be stationary over the entire trace. However, this is an approximation; as shown in Fig. 1, some traces are non-stationary, for example the average SNR changes over time. Still, in Section 5.4 we show the impact of this assumption on the accuracy in predicting the performance of HARQ. In such a setup, also the computed SNR average can be re-scaled by adding or subtracting a constant value (in dB). This corresponds to changing the source power level of the transmitters, assuming that non-idealities of the receiver, such as intersymbol interference due to reverberation, are either negligible or scale identically.

3.3. Quantization of the channel quality

Even when the channel statistics are available, evaluating the outcome of an HARQ packet transmission for IR-HARQ would require to track a k -tuple of SNR values (one per transmission). Since the SNR is continuous, this would require to evaluate infinitely many values k times, which is of course impossible. This problem can be simplified by establishing a proper quantization that leads to modeling the channel as a FSMC. In particular, we employ a Markov representation of order 1, since [23] shows that a Markov model of order N can be simplified to one with a smaller order for different fading parameters, without loss of accuracy in representing the channel quality statistics.

On top of the reliability region model, we construct a channel model following the guidelines for channel state quantization described in [20], and briefly summarized in the following. Before channel quantization, a vector of channel states has the form $\mathbf{s}^{(k)}$, as defined above, where each element can take infinitely many values in \mathbb{R} . Quantization of the channel states maps $\mathbf{s}^{(k)}$ into a k -tuple of discrete values, that evolve according to an FMSC. If N thresholds $\alpha_1, \dots, \alpha_N$ divide \mathbb{R} into $N+1$ intervals I_0, \dots, I_N , where $I_j = [\alpha_j, \alpha_{j+1}]$, and we define $\alpha_0 = 0$ and $\alpha_{N+1} = +\infty$, any real value is mapped into the discrete index j of the interval I_j it falls within. To formalize this mapping, define $d(s_k)$ as the function returning the

interval of \mathbb{R} where s_k is contained, i.e., $d(s_k) = j$ if $s_k \in I_j$. By grouping the mappings for all elements of an SNR k -tuple $\mathbf{s}^{(k)}$ into a vector, we can write $\mathbf{d}^{(k)} = (d(s_1), \dots, d(s_k))$, thereby establishing a map between every k -tuple $\mathbf{s}^{(k)}$ and an element of the set \mathbb{Z}_{N+1}^k , where $\mathbb{Z}_{N+1} = \{0, 1, \dots, N\}$. Vector $\mathbf{d}^{(k)}$ represents the fact that $\mathbf{s}^{(k)} \in I_{d(s_1)} \times I_{d(s_2)} \times \dots \times I_{d(s_k)} \subset \mathbb{R}^k$.

An FSMC channel model entails the assumption that the statistics of the SNR has the Markov property, a common means of describing correlated SNR evolution over time [10,24]; the model parameters can then be derived from the distribution of the SNR. If the pdf of the SNR, γ , is called $f_\Gamma(\gamma)$, the state space of the channel is \mathbb{Z}_{N+1} , and the steady-state distribution is

$$\pi_i = \int_{\alpha_i}^{\alpha_{i+1}} f_\Gamma(\gamma) d\gamma, \quad i = 0, \dots, N. \quad (2)$$

Analogously, the probability t_{ij} of a transition between states i and j can be derived as

$$t_{ij} = \frac{\int_{\alpha_i}^{\alpha_{i+1}} f_\Gamma(\gamma_0) \int_{\alpha_j}^{\alpha_{j+1}} f_\Gamma(\gamma|\gamma_0) d\gamma d\gamma_0}{\int_{\alpha_i}^{\alpha_{i+1}} f_\Gamma(\gamma_0) d\gamma_0}, \quad i, j \in \mathbb{Z}_{N+1}, \quad (3)$$

where $f_\Gamma(\gamma|\gamma_0)$ is the conditional pdf of the SNR γ given the previous SNR value γ_0 .

The channel transition probability matrix is then defined as $\mathbf{T} = (t_{ij})$ for $i, j \in \mathbb{Z}_{N+1}$. We directly estimate the channel transition probabilities from the data, by estimating the relative frequencies of SNR transitions between any two intervals I_i, I_j , with $i, j \in \mathbb{Z}_{N+1}$.

It is worth noting that the transition probabilities strongly depend on the number of states used to quantize the channel, and therefore on the number of thresholds delimiting the SNR intervals (or, equivalently, SNR probability intervals). In this paper, we will employ only two thresholds, resulting in a total of three channel states. This choice results in a very simple channel model, but still provides sufficient quantization accuracy, as shown by the numerical results.¹

4. Models for HARQ schemes

We now specify how the previously FSMC channel model is employed in the analytical model of the HARQ error control process, based on good LDPC code ensembles. Recall that \mathbf{T} denotes the transition probability matrix of the FSMC. The FSMC has in general $N+1$ states $0, 1, \dots, N$, if N thresholds are chosen to quantize the channel behavior. With no loss of generality, assume that 0 is the best state, i.e., the one associated to the highest values of the SNR, whereas N is the worst state. Following the model developed in [20], we define a map $g(\cdot)$ which associates each state index j , $j = 0, \dots, N$, to the “error level” of a packet transmitted while the channel is in state j . The

¹ Note that, in general, a large number of states may be needed to accurately represent a fading channel. However, in our approach we jointly consider the quantization of the fading gain and the corresponding threshold for the ARQ success/failure events. Matching the quantization intervals to the ARQ threshold leads to a very accurate model with very few states [20].

error level is a non-decreasing function of the state index, and is employed to describe the usefulness of the packet being transmitted for the decoding of the LDPC codeword at the receiver as follows. As explained in Section 3, every information frame is encoded and divided in HARQ fragments, to be transmitted sequentially, and each correctly received HARQ fragment is sufficient to successfully decode the whole information frame. However, corrupted fragments may still be used at the receiver. A successful decoding takes place after reception of HARQ fragment k only if the overall error level (which is defined as the error level of fragment k for Type I HARQ, and as the sum of the error levels of all HARQ fragments received so far for IR-HARQ) is lower than or equal to a certain threshold θ_k .

With the above in mind, and for a given SNR statistics over the link, the performance of the HARQ scheme depends on the channel round-trip time, measured in slots, m , and on the maximum number of transmissions allowed before an information frame is discarded, denoted by F [13]. As mentioned in Section 3.2, our data set contains transmissions performed once every 15 s, which is larger than the maximum round-trip time spanning the distances between the transmit and receive hardware. Therefore, we set $m = 1$ for our data set, which corresponds to assuming that a slotted approach is taken, whereby each slot is long enough to accommodate the maximum round-trip time and the time required for acoustic reverberation to fade out. Note that setting $m = 1$ means that the transmitted frames are actually sent only after receiving the ACK/NACK related to the previous message, so that at every time instant there is at most one message in flight over the channel (i.e., the ARQ scheme is Stop-and-Wait, or alternatively it may be seen as an *ideal* ARQ). This does not limit the validity of our approach, which can be extended to higher values of m by following [13].

Finally, in order to keep the discussion simple, we assume that each corrupted packet can be retransmitted only once, i.e., $F = 2$, and if the retransmission fails the packet is discarded. Note that this assumption is justified by several considerations, including the limited storage capabilities of practical devices [4], and in many realistic contexts is not very limiting. For example, in sensing applications, due to the long delay of the underwater channel, it may be considered efficient to try another transmission attempt of an erroneous packet (with higher delivery probability than the first one), but after two transmission attempts it may be more convenient to start anew and transmit a fresh packet with more recent data instead. In addition, we numerically found this choice to be justified also by the concrete setup of our scenarios, including that the practical underwater channel is correlated, and therefore a third transmission attempt may not be very useful if the first two already failed. The interested reader is referred to Appendix A for the related numerical analysis, obtained by simulating the HARQ procedures over the channel traces.

To evaluate Type I and Type II HARQ we need a model that at each time instant keeps track of the number of retransmissions already made and the correspondingly accumulated error level, as well as of the channel state. In our specific case, where $F = 2$, $m = 1$, $N = 2$, the model

is relatively easy to solve in closed-form; nevertheless, as shown by the numerical results, it fits well the scenarios considered.

4.1. Type II (Incremental Redundancy) HARQ

We start with the description of the Type II HARQ (IR-HARQ) scheme. If we employ $N = 2$ thresholds to describe the channel behavior, the model of [20] results in three channel states, namely 0 (error-free state), 1 (some recoverable errors), 2 (worst state with unrecoverable errors). In general, each state j is associated to a different error level incurred by a fragment transmitted when the channel is in that state through the map $g(j)$. For our three state model, following [13] it can be shown that $g(j) = j$, i.e., the label of each state also represents its error level.

As another consequence of the model, if the transmission of the first fragment occurs when the channel is in state 0 (error-free state), the frame is correctly received and no retransmission is needed. If instead the first fragment is in error, a new fragment is transmitted, and the frame can still be recovered if the states over the two attempts are 1–0, 1–1 or 2–0. Instead, the model dictates that states 2–1, 1–2, and 2–2 are the cases that do not lead to successful frame recovery. In other words, the model dictates that the sum of the indices must be less than or equal to 2 for the packet to be corrected. This approach shares some similarities with the concept of accumulated mutual information [25].

Therefore, we represent the system state with an ordered pair of variables (S, r) , where S is the previous channel state (required to track the evolution of the Markov channel) and r denotes the number of transmissions already made for the current frame, i.e., $r = 0$ for the first fragment and $r = 1$ for a retransmission. There is no need for an explicit variable tracking the error level of the packet, as it is identical to S . Note also that there are only *five* possible states (S, r) , although S and r can take three and two values, respectively. Indeed, combination $S = 0$, $r = 1$ is invalid as it would correspond to the retransmission of a correctly received frame. The resulting five-state Markov chain is easily solvable by observing that only three outgoing transitions are possible from each state.

Thus, define $\sigma_{S,r}$ as the steady-state probability of being in state (S, r) . If t_{ij} denotes the probability of making a transition from channel state i to state j , the balance equations between such steady-state probabilities can be found as

$$\sigma_{00} = \sum_{i=0}^2 \sigma_{i0} t_{i0} + \sum_{i=1}^2 \sigma_{i1} t_{i0}, \quad (4)$$

$$\sigma_{S0} = \sum_{i=1}^2 \sigma_{i1} t_{iS} \quad \text{for } S = 1, 2, \quad (5)$$

$$\sigma_{S1} = \sum_{i=0}^2 \sigma_{i0} t_{iS} \quad \text{for } S = 1, 2. \quad (6)$$

All these equations impose a steady-state condition on the Markov states. For example, state 00 describes the case of a packet transmitted for the first time after the previous packet was correctly received, because the channel was good. Thus, σ_{00} is found by considering the transitions

from all possible states (which are five, since there is no state with $S = 0$ and $r = 1$), towards a channel in state 0. The probabilities that the previous channel state is $S \in \{1, 2\}$, i.e., the channel is not fully correct, are derived as follows: in the case $r = 1$, the probability is σ_{s_1} and the packet is currently retransmitted, so at the previous time slot it must have been at its first transmission, i.e., $r = 0$. Conversely, if the present value of r is 0, the probability is σ_{s_0} and the current packet is at its first transmission, thus the previous packet was at its last transmission attempt.

These equations can be put into a system that can be solved by imposing the additional condition that the sum of all σ_{s_r} equals 1. After solving the system, one can directly compute the throughput, Θ (average number of successful frames per slot), the average number of retransmissions per correctly decoded information frame, N_{fr} , and the probability that a frame is discarded, P_{fd} (i.e., the fraction of frames that are not correctly received), as

$$\Theta = \sum_{i=0}^2 \sigma_{i0} t_{i0} + \sum_{i=1}^2 \sigma_{i1} t_{i0} + \sigma_{11} t_{11} = \sigma_{00} + \sigma_{11} t_{11}, \quad (7)$$

$$N_{fr} = \frac{\sigma_{11} t_{10} + \sigma_{11} t_{11} + \sigma_{21} t_{20}}{\sum_{i=0}^2 \sigma_{i0} t_{i0} + \sum_{i=1}^2 \sigma_{i1} t_{i0} + \sigma_{11} t_{11}} = \frac{\sigma_{11} (t_{10} + t_{11}) + \sigma_{21} t_{20}}{\Theta}, \quad (8)$$

$$P_{fd} = \frac{\sum_{i=0}^2 \sigma_{i0} (t_{i1} t_{i2} + t_{i2} (1 - t_{20}))}{\sum_{i=0}^2 \sigma_{i0}}. \quad (9)$$

These three metrics describe different quality parameters of the communication: while Θ can be seen as a measure of the amount of transmitted data, P_{fd} quantifies how much data are lost, and finally N_{fr} is a measure of delay. Eqs. (7)–(9) directly come from the balance equations. The throughput in (7) is derived by summing the probabilities of all transitions where a frame is successful, which include all transmissions in channel state 0, plus the case where a retransmission in state 1 follows an erroneous transmission that was itself in state 1; also, note the simplification as per the balance Eq. (4). Eq. (8) is again obtained by enumerating all events that correspond to the successful delivery of a frame in a slot: the sum of the probabilities of these events equals the throughput Θ and is the denominator of (8), whereas the numerator sums the probabilities of only those events that correspond to a success after retransmission. Finally, (9) is derived by conditioning on the case that the first transmission of the packet (thus, $r = 0$) occurs after the channel has been in a generic state S , and considering all possible transitions leading to the packet being discarded, i.e., $S \rightarrow 1 \rightarrow 2, S \rightarrow 2 \rightarrow 1, S \rightarrow 2 \rightarrow 2$.

4.2. Type I HARQ

As a term of comparison, we also consider a Type I hybrid HARQ where only one HARQ fragment is considered at every decoding attempt and no packet combining is employed: further retransmissions can help the decoding process only by providing higher chances to incur a sufficiently high SNR value through time diversity. This entails the definition of a single threshold, thus leading to two cases: if the SNR is above the threshold, the frame is

correctly decoded; otherwise, it is retransmitted once; if, again, the SNR threshold is not met, the frame is discarded. For a fair comparison with Type II, we keep the maximum number of transmissions as $F = 2$.

Type-I HARQ can be modeled using the same set of balance Eqs. (7)–(9) as before. While the same solution approach is kept, we do not include incremental redundancy, i.e., two subsequent transmissions of the same frame that both experience channel state 1 no longer yield a correct decoding. In this way, any term related to this event is to be counted as a failure. Thus,

$$\Theta = \sigma_{00}, \quad (10)$$

$$N_{fr} = \frac{\sigma_{11} t_{10} + \sigma_{21} t_{20}}{\Theta}, \quad (11)$$

$$P_{fd} = \frac{\sum_{i=0}^2 \sigma_{i0} (t_{i1} (1 - t_{10}) + t_{i2} (1 - t_{20}))}{\sum_{i=0}^2 \sigma_{i0}}. \quad (12)$$

We remark that this model of Type-I HARQ is practically relevant, as it properly describes the behavior of current underwater acoustic modems, which typically include a form of physical-layer FEC hardcoded in the modem firmware, on top of which ARQ is independently provided by the modem users, yielding a Type-I HARQ system without packet combining.

5. Performance results

We present the results obtained by employing experimental data in the analytical framework discussed so far. In particular, we analyze the critical points of the framework (quantization, statistical correlation and independence of subsequent SNR, model validation) by evaluating the metrics considered for HARQ: average throughput Θ , average number of HARQ fragments per correctly decoded frame N_{fr} and frame discarding probability P_{fd} .

We aim at showing the applicability of the described framework by focusing on: (i) a comparison of HARQ I and II for different underwater acoustic links; (ii) the quantization error; (iii) the performance analysis with independent and correlated subsequent SNR values; (iv) the validation of the Markov model. These results provide evidence that the proposed framework can be applied to the evaluation of HARQ for communications in underwater scenarios.

All the results are plotted as a function of the average SNR, which is computed over the whole time series. Different values of the average SNR are obtained by re-scaling the whole SNR trace, thus maintaining the temporal fluctuations shown in Fig. 1. This approach corresponds to assuming a re-scaled source level for transmissions, as discussed in Section 3.2.

5.1. Performance results obtained by simulation over different links

We compare the results obtained by using the SNR traces, collected over the different links represented in Fig. 1, i.e., from transmitters T1, T2, and T3 to receiver H2. This means that (see Section 3.2) three transmitters

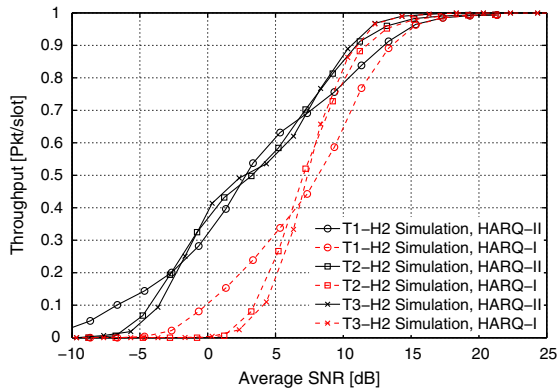


Fig. 2. θ vs. the average SNR in dB, obtained by simulation for different stationary underwater acoustic links. Dashed/solid lines refer to Type I/Type II HARQ, respectively. Different markers correspond to different links.

located at different distances, with T3 being the closest and T2 the farthest, communicate with the same receiver placed 40 m below the surface. The employed LDPC encoder has coding rate 1/5. Figs. 2–4 show throughput, number of transmitted frames and probability of frame discarding, respectively, for Type I and Type II HARQ.

From Figs. 2–4, we can also observe how the different dynamics of the channel quality affect the trend of the curves. For example, in Fig. 2, link T3–H2 is characterized by the steepest throughput curve for both Type II and I HARQ, since it also exhibits smaller fluctuations around the average SNR, as shown in Fig. 1. For the same reason, in low SNR regimes, the shortest link (T3–H2) has poorer performance than longer ones, whereas in high SNR regimes, the T3–H2 link has the highest throughput. Moreover, Type II HARQ mitigates this effect for SNR between -2 and 7 dB, since it exploits incremental redundancy.

These results provide insight on how to practically deploy the network in case HARQ techniques are employed. If the system operates in low average SNR regimes (in this case from -5 to 6 dB), then links with wider dynamics are preferable, especially for HARQ Type I. In high average SNR regimes (here, above 7 dB) the links with more limited dynamics have better performance. As shown in this data set, the stability of a link is not a monotonic function of its length. In fact, the link at 1500 m has wider fluctuations than the ones at 2200 m and 700 m (see Fig. 2). The channel corresponding to the longest link consists of fewer surface reflected arrivals, given that their energy might be absorbed or dispersed before reaching the receiver.² The stability of the shortest link is mainly due to the presence of a strong line-of-sight path. Link T1–H2 appears to be often the “worst” or at least the “least stationary” of the three; hence, we concentrate most of our attention on it.

² Other causes of SNR fluctuation, such as time-varying surface conditions, changing sound speed profile or water inhomogeneities, would likely affect all links in the same way, given that they are deployed in the same area.

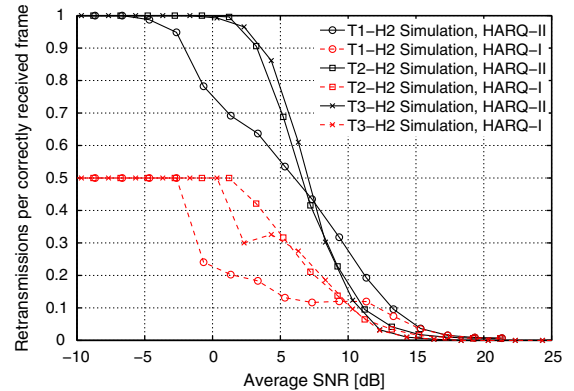


Fig. 3. N_{fr} vs. the average SNR in dB, obtained by simulation for different stationary underwater acoustic links. Dashed/solid lines refer to Type I/Type II HARQ, respectively. Different markers correspond to different links.

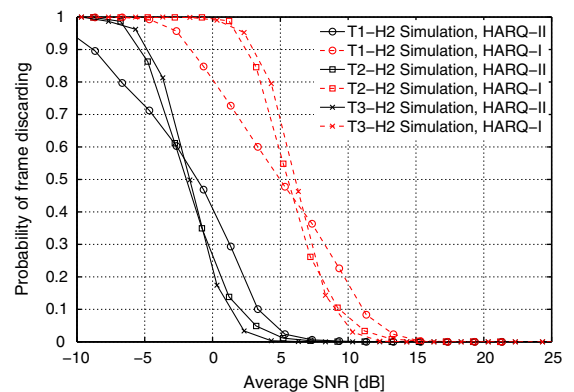


Fig. 4. P_{fd} vs. the average SNR in dB obtained by simulation for different stationary underwater acoustic links. Dashed/solid lines refer to Type I/Type II HARQ, respectively. Different markers correspond to different links.

Fig. 3 shows a further difference between Type I and Type II HARQ: as long as the average SNR is low, the average number of retransmissions incurred by Type I is 0.5 , whereas that of Type II is 1 . Recall that N_{fr} is the average number of retransmissions experienced by a *correctly decoded* information frame. When channel conditions are unfavorable, the event of correct decoding is so rare that Type I HARQ experiences a success at the first or the second transmission of a fragment with equal probability, which leads to an average of 1.5 transmissions per successfully received packet ($N_{fr} \approx 0.5$). With Type II HARQ, the transmission of a second fragment always improves the decoding performance, so that successful decoding after the retransmission is significantly more likely, and most correctly received frames need two transmissions and $N_{fr} \approx 1$. To better understand this result, it may be useful to compare it with Fig. 4, where the frame discarding probability is shown. Type II HARQ discards much fewer frames than Type I, leading to an overall lower average number of retransmissions, if all the packets (not just those which are correctly received) are included.

5.2. Effect of the quantization error

In Figs. 5–7 we present the results, again obtained by simulation, for HARQ Type II over link T1–H2, when we use quantized reliability regions. These results show how accurately we can assess the system performance by

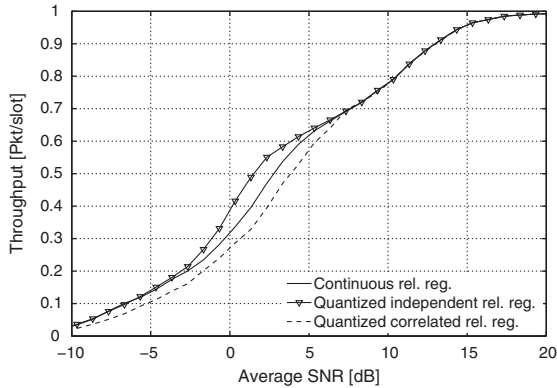


Fig. 5. Θ vs. the average SNR in dB for Type II HARQ (simulated) for different representations of the reliability region.

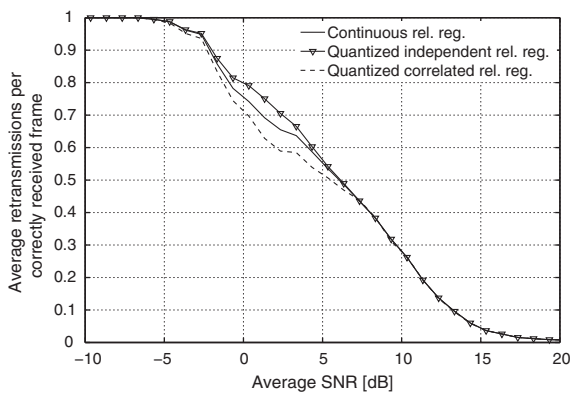


Fig. 6. N_{tr} vs. the average SNR in dB for Type II HARQ (simulated) for different representations of the reliability region.

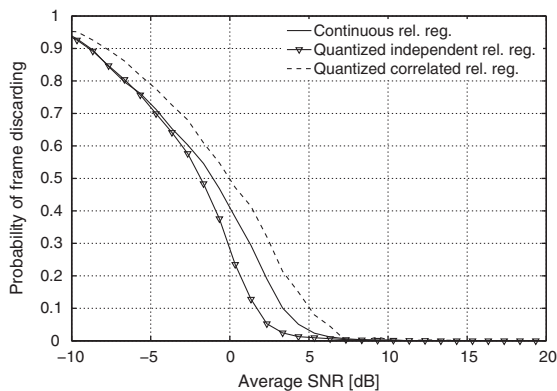


Fig. 7. P_{rd} vs. the average SNR in dB for Type II HARQ (simulated) for different representations of the reliability region.

relying on the quantization criteria studied in [20]. Since the reliability region for HARQ Type I is one-dimensional, we only consider the performance of HARQ Type II, which instead is characterized by a bi-dimensional reliability region.

In the following, we assume that the SNRs of the first and second transmission of an information frame are: (i) independent, or (ii) correlated. In the former case, we can employ the quantization method in [20], i.e., we compute the corresponding reliability region in the probability density functions space, by assuming a normal distribution of the SNRs, which accurately fits the time series as shown in [1]. In the latter case, the reliability region, and consequently its quantization, is recomputed according to [20], where, however, we use joint probability density functions of correlated random variables. Figs. 5–7 show the effect of the quantization error on the performance evaluation. Inaccuracy in predicting all metrics occurs for SNR values smaller than 7 dB, where throughput is also lower than 0.7, thus representing an SNR regime with relatively poor communication performance. Moreover, for SNR less than -2 dB, the throughput and probability of frame discarding are more sensitive to the quantization error than the number of retransmissions. In fact, at very low SNR, N_{tr} is independent of how the small reliability region is quantized, since a retransmission is always requested. When subsequent SNR values are assumed to be independent, the performance of the HARQ scheme is slightly overestimated, since the reliability regions are larger than those for the correlated case.

5.3. Performance results obtained by analysis by assuming independent and correlated SNRs

In Figs. 8–10 we present the results of the analysis based on the Markov model in Section 4, and we compare these curves with those computed by simulation. In particular, the label “ind” (“corr”) refers to the analytical results for an independent identically distributed (time-correlated) channel model for both the derived Markov chain and the quantization of the reliability region. Instead, the label “independent” to the curves obtained by simulation

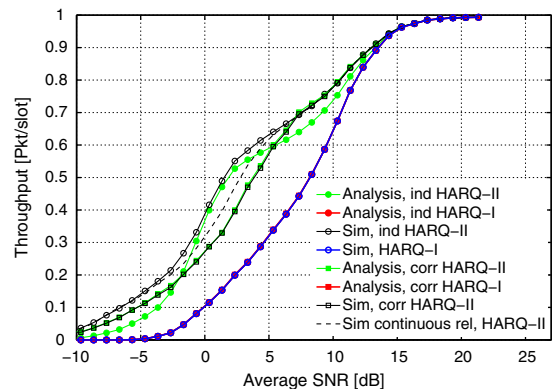


Fig. 8. Average throughput obtained by simulation and analysis (filled markers) for Type II and Type I HARQ over link T1–H2. The black dashed curve represents the results for the continuous reliability region.

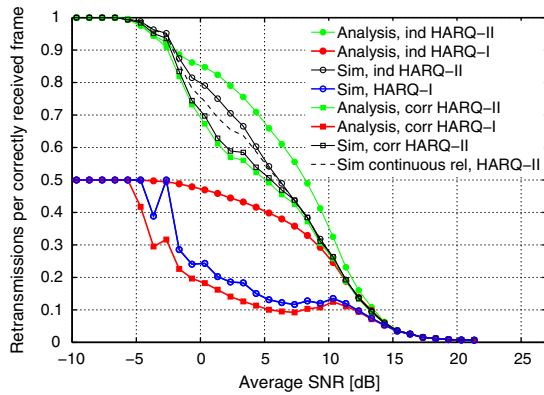


Fig. 9. Average number of retransmissions obtained by simulation and analysis (filled markers) for Type II and Type I HARQ over link T1–H2. The black dashed curve represents the results for the continuous reliability region.

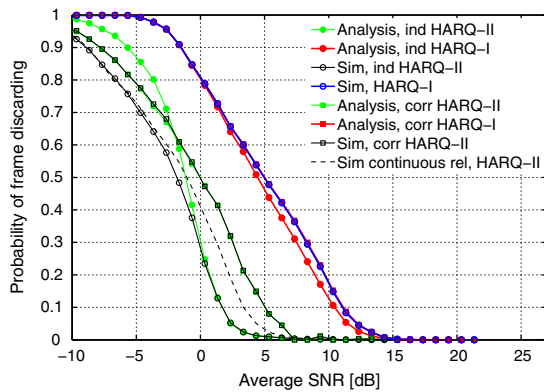


Fig. 10. Probability of frame discarding obtained by simulation and analysis (filled markers) for Type II and Type I HARQ over link T1–H2. The black dashed curve represents the results for the continuous reliability region.

corresponds only to the assumption used to quantize the reliability region. Note that we show only one curve representing the results computed by simulation for HARQ Type I, since in this case no quantization is performed on the one-dimensional reliability region. Figs. 9 and 10 show that the independent channel model is less accurate than the correlated one. This suggests that time-correlation should be suitably represented by any channel model, when HARQ schemes are evaluated in UWA communications, since this has an impact on the performance. Instead, when the Markov chain represents a correlated channel model the analytical and simulation results show a better match, thus suggesting that the FSMC model can suitably describe the underwater acoustic channel correlated time evolution. We recall that in these cases the simulation results are computed by using the quantized reliability regions, whereas only the black dashed line corresponds to the simulation without quantizing the reliability regions. Fig. 9 exhibits a slight mismatch (less than 10%) between analysis and simulations in the middle SNR regime for Type II HARQ. This is due to loss of accuracy

in estimating the steady-state probabilities of the FSMC states that describe a retransmission event. Indeed, a retransmission rarely occurs when the average SNR is around 5 dB, thus leading to bad estimates, whereas it becomes more likely as the average SNR decreases, and therefore the mismatch is reduced. Throughput and probability of frame discarding are less sensitive to these fluctuations, since these metrics are related to the successful delivery of an information frame, and therefore the steady-state probabilities are always accurately estimated. We also note a mismatch between analytical and simulation results for Type I HARQ in Fig. 9 when SNR values are lower than 0 dB. This is caused by the inaccuracy of estimating N_{fr} in simulations for low throughput values.

5.4. Model validation

In all the plots above, the simulation results match the analysis fairly accurately in most cases. This is a consequence of having the training set equal to the test set, i.e., we trained the Markov models over the full SNR traces, and we also performed simulation runs over the same traces. In this subsection, we validate the accuracy of the models by training the model over a different portion of the data set than used in the simulations. Our purpose is also to test the validity of the assumption that the SNR process is stationary, which is implicitly made when we estimate the transition probabilities of the Markov channel model. Actually, real underwater channel traces may exhibit significantly non-stationary behavior and therefore it is critical to test if our model is still applicable in these cases.

Again, we show the results only for link T1–H2, which is the worst trace where to infer the statistics of the Markov model from the experimental data, as it is not really stationary; the other traces yield similar or better results. Moreover, we focus only on Type II HARQ, given that it outperforms Type I HARQ and therefore looks more interesting. Finally, for the sake of conciseness, we just plot the results for the throughput, but the other metrics were also investigated and gave analogous results.

We considered, for Type II HARQ, the absolute error between the actual results and what predicted by the model, i.e., the (signed) difference between the “sim” and the “analysis” values in Figs. 8–10, where the model is trained only on a fraction of the full series. If the length of the time series (9 h) is T , we consider the following cases: (i) the model is trained on the first half of the trace $[0, T/2]$, and both analytical and simulation results are on the second half of the trace, i.e., on $[T/2, T]$; (ii) the model is trained on the first quarter of the trace $[0, T/4]$ and the results are on the remaining three quarters of the trace, i.e., on $[T/4, T]$; (iii) the model is trained over the initial 1/16 of the trace, then numerical results are evaluated over the subsequent quarter of the trace, i.e., on $[T/16, 5T/16]$; after that, the model is retrained on the last interval of $T/16$ duration, i.e., $[T/4, 5T/16]$ and the retrained model is evaluated on $[5T/16, 9T/16]$ and so on. Cases (i) and (ii) are also investigated with a re-scaling procedure of the SNR, as discussed below.

The results are shown in Fig. 11. When the model was trained over the full trace, a very good match between

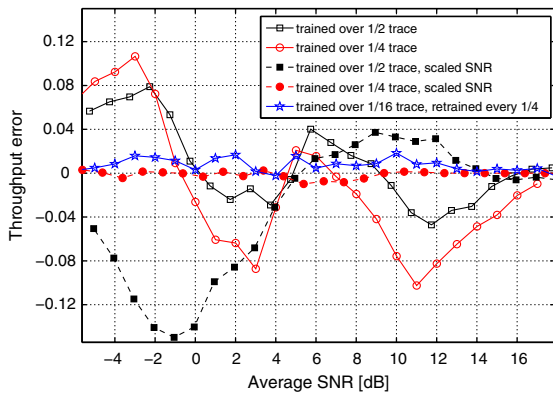


Fig. 11. Absolute error of the throughput when the model is trained and evaluated on different parts of the time series, i.e., trained in the first half/quarter and evaluated in the rest. Also including a re-scaling procedure for the SNR and a retraining case with training over 1/16 of the series and retraining every quarter.

analysis and simulation was obtained, and the absolute error was below 0.01. Here, we see a larger absolute error in the evaluations for the partial trainings; still, in most of the cases the estimate is reliable enough (in the worst cases the error is slightly above 0.1). Therefore, the throughput evaluation may still be empirically acceptable. The reason of this bias in the evaluation lies in non-stationarity of the traces, the largest evidence of which is the difference in the average SNR among different portions of the series. In particular, we remark that the average SNR can be different when the model is trained and when it is used to evaluate the performance; incidentally, this means that when plotting the error curves, the simulation value should refer to a different point on the x -axis. However, our model itself allows for re-scaling the SNR (we already used this feature when plotting the previous figures). Thus, we consider a better way to use the partially trained model by computing the difference between the simulation and analytical results for cases (i) and (ii) but at the same time re-scaling the simulated value to the correct average SNR value; such values are those plotted with “filled-markers” in Fig. 11. With such an approach the error decreases if the training phase is short enough (apparently, in this case the wrong SNR estimate is filtered out³), to the point that the shorter training performs better than the longer one, contrary to the previous comparison.

Scaling the SNR requires to know its average value, which is generally not available a priori. Another solution would be to periodically retrain the model, whenever a significant change of the channel behavior is observed. This is supported by the result of case (iii), which evidently achieves good performance, with the absolute error always below 0.02. We remark that in case (iii) the training phase still lasts more than 33 min, i.e., long enough to collect significant statistics. In a real setup, further refinements

³ This happens in spite of our model *not considering* the SNR average value directly, but only the quantization thresholds and the transition probabilities from one state to another.

would be possible by persistently taking measurements and filtering them, e.g., with a moving window approach.

6. Conclusions

In this paper, we presented a methodology for evaluating the data-link layer in underwater acoustic networks including error control via HARQ schemes. To this end, we analyzed an experimental data set, we included some contributions in the literature in order to derive an original evaluation framework, and we validated it through experimental data. Our approach consisted in estimating the channel statistics, deriving the corresponding reliability regions of the HARQ scheme, quantizing the channel quality in order to obtain a FSMC, and evaluating the performance of HARQ schemes. The employed statistical model has been shown to significantly simplify channel representation, yet to satisfactorily adhere to the actual channel behavior. Thus, the performance of HARQ policies can be characterized with low complexity, even in the presence of a dynamic behavior of the channel, provided that proper countermeasures (e.g., fitting or retraining the model) are taken to make it consistent with the scenario.

The present framework can be applied to the design of a reliable data-link layer through HARQ schemes for underwater communications. Avoiding the need for collecting the entire data trace and/or implementing a testbed, the model can be used for an analytical and modular evaluation of coding schemes and/or required power of the transmitter. From a networking perspective, given its relatively low space- and time-complexity, the above framework can be integrated within theoretical optimization models, as well as used for the design and validation of communication protocols with quality requirements. In the context of cross-layer optimization, it can be even coupled with network layer design for the evaluations of underwater network deployments and/or path selection.

Appendix A

Underwater channels are characterized by very large delays, and therefore HARQ schemes with more than one retransmission may often be impractical. This is the main reason why, even though a more general approach could have been adopted following [13], we focused on a single retransmission in our analysis, which has the additional benefit of resulting in simple closed-form expressions. In order to further support the validity of this choice, in this appendix we compare the performance of the considered system when 2 and 3 transmissions (i.e., with 1 and 2 retransmissions) are allowed. More specifically, Figs. 12 and 13 report the throughput and the average number of retransmissions, respectively, experienced by correct packets. Although the results reported here are just an example for a specific configuration, other similar evaluations were found to be entirely in line with this one.

If we look at Fig. 12 and consider only the region where throughput is higher than 0.5 as a practical operation regime, we see that there is almost no visible enhancement. Larger relative gains can be observed in the low

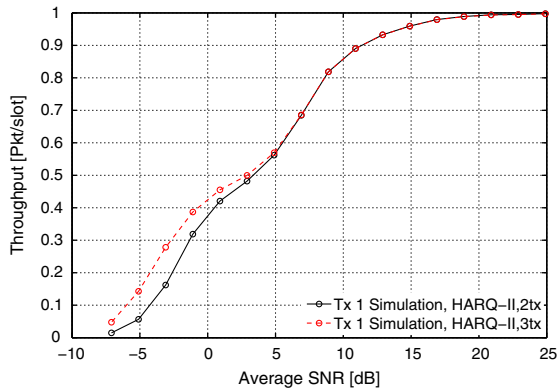


Fig. 12. Θ vs. the average SNR in dB for Type II HARQ (simulated) for different numbers of retransmissions.

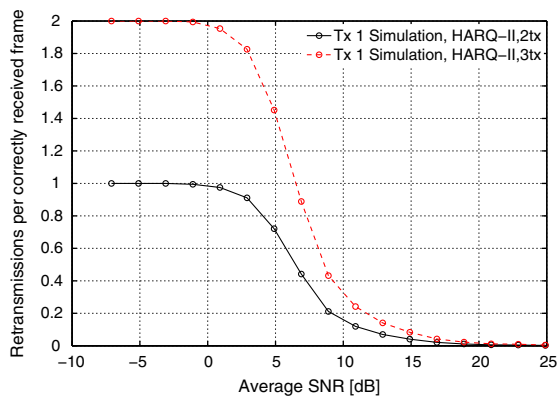


Fig. 13. N_{fr} vs. the average SNR in dB for Type II HARQ (simulated) for different numbers of retransmissions.

SNR regime, which on the other hand corresponds to very small throughput values and therefore can be considered of lesser practical interest.

In addition, there is a heavy price to pay for these marginal throughput improvements, as shown in Fig. 13: in all the cases where the throughput is increased, the average number of retransmissions is doubled, which causes a significant degradation in terms of both delay and energy consumption. These results provide support to our previous claim that assuming a single retransmission is not a significant limitation for the scenarios considered.

References

- [1] B. Tomasi, P. Casari, L. Badia, M. Zorzi, A study of incremental redundancy hybrid ARQ over Markov channel models derived from experimental data, in: Proc. of ACM WUWNet, October 2010.
- [2] J. Heidemann, W. Ye, J. Willis, A. Syed, Y. Li, Research challenges and applications for underwater sensor networking, in: Proc. of the IEEE Wireless Communications and Networking Conference, April 2006.
- [3] J. Partan, J. Kurose, B. Levine, A survey of practical issues in underwater networks, in: Proc. of ACM WUWNet, Los Angeles, CA, September 2006.
- [4] S2CR 18/34 WiSE underwater acoustic modem. <http://www.evologics.de/en/products/developer_tools/S2CR_18_34_WiSE.html> (accessed 31.05.14).

- [5] B. Tomasi, P. Casari, L. Finesso, G. Zappa, K. McCoy, M. Zorzi, On modeling JANUS packet errors over a shallow water acoustic channel using Markov and hidden Markov models, in: Proc. IEEE MilCom, November 2010, pp. 2406–2411.
- [6] M. Siderius, M.B. Porter, P. Hursky, V. McDonald, the KauaiEx Group, Effects of ocean thermocline variability on noncoherent underwater acoustic communications, *J. Acoust. Soc. Am.* 121 (4) (2007) 1895–1908.
- [7] P. Qarabaqi, M. Stojanovic, Statistical modeling of a shallow water acoustic communication channel, in: Proc. of IACM UAM, Nafplion, Greece, 2009.
- [8] M. Chitre, J. Potter, O.S. Heng, Underwater acoustic channel characterisation for medium-range shallow water communications, in: MTS/IEEE OCEANS, 2004.
- [9] B. Tomasi, G. Zappa, K. McCoy, P. Casari, M. Zorzi, Experimental study of the space-time properties of acoustic channels for underwater communications, in: Proc. IEEE/OES Oceans, Sydney, Australia, 2010.
- [10] Q. Zhang, S.A. Kassam, Finite-state Markov model for Rayleigh fading channels, *IEEE J. Sel. Areas Commun.* 17 (5) (1999) 867–880.
- [11] E. Soljanin, N. Varnica, P. Whiting, Punctured vs. rateless codes for hybrid ARQ, in: Proc. of IEEE ITW, Punta del Este, Uruguay, March 2006, pp. 155–159.
- [12] R. Liu, P. Spasojevic, E. Soljanin, Reliable channel regions for good binary codes transmitted over parallel channels, *IEEE Trans. Inf. Theory* 52 (4) (2006) 1405–1424.
- [13] L. Badia, M. Levorato, M. Zorzi, Markov analysis of selective repeat type II hybrid ARQ using block codes, *IEEE Trans. Commun.* 56 (9) (2008) 1434–1441.
- [14] M. Stojanovic, Optimization of a data link protocol for underwater acoustic networks, in: Proc. MTS/IEEE OCEANS, September 2005.
- [15] J.-W. Lee, J.-P. Kim, J.-H. Lee, Y.S. Jang, K.C. Dho, K. Son, H.-S. Cho, An improved ARQ scheme in underwater acoustic sensor networks, in: Proc. MTS/IEEE OCEANS, September 2008.
- [16] M. Gao, W.-S. Soh, M. Tao, A transmission scheme for continuous ARQ protocols over underwater acoustic channels, in: Proc. IEEE ICC, June 2009, pp. 1–5.
- [17] L. Badia, P. Casari, M. Levorato, M. Zorzi, Analysis of an automatic repeat request scheme addressing long delay channels, in: Proc. IEEE WAINA, 2009, pp. 1142–1147.
- [18] W.-Y. Shin, D.E. Lucani, M. Médard, M. Stojanovic, V. Tarokh, Multi-hop routing is order-optimal in underwater extended networks, in: Proc. IEEE Int. Symp. on Information Theory Proceedings (ISIT), 2010, pp. 510–514.
- [19] A. Ghosh, J.-W. Lee, H.-S. Cho, Throughput and energy efficiency of a cooperative hybrid ARQ protocol for underwater acoustic sensor networks, *Sensors* 13 (11) (2013) 15385–15408.
- [20] L. Badia, M. Levorato, M. Zorzi, A channel representation method for the study of hybrid retransmission-based error control, *IEEE Trans. Commun.* 57 (7) (2009) 1959–1971.
- [21] Teledyne benthos undersea systems. <<http://www.benthos.com>>.
- [22] S. Lin, D.J. Costello, *Error Control Coding: Fundamentals and Applications*, Prentice-Hall, 1983.
- [23] F. Babich, G. Lombardi, A Markov model for the mobile propagation channel, *IEEE Trans. Veh. Technol.* 49 (1) (2000) 63–73.
- [24] F. Babich, On the performance of efficient coding techniques over fading channels, *IEEE Trans. Wireless Commun.* 3 (1) (2004) 290–299.
- [25] G. Caire, D. Tuninetti, The throughput of hybrid-ARQ protocols for the Gaussian collision channel, *IEEE Trans. Inf. Theory* 47 (5) (2001) 1971–1988.



Beatrice Tomasi received the PhD in Information Engineering in 2011 at the University of Padova, Italy, where she was a postdoctoral research fellow during 2012. She has been actively working on underwater acoustic channel modeling and the performance evaluation of communication systems and networking protocols for underwater acoustic networks. She was a visiting student at the NATO Undersea Research Center (NURC, today CMRE) during 2009 and at the Woods Hole Oceanographic Institution (WHOI) in 2011,

where she is currently a postdoctoral research fellow. She actively participated in the Italian project NAUTILUS, and was involved in research efforts funded by the European Community. Her research interests include energy efficient protocol for underwater acoustic networks and

their impact on marine mammals.



Paolo Casari received the PhD in Information Engineering in 2008 at the University of Padova, Italy, where he is currently a post-doctoral research fellow. He has been actively researching cross-layer protocol design for MIMO ad hoc networks and wireless sensor networks. After spending a period at the Massachusetts Institute of Technology in 2007, he started working on underwater acoustic networks, which is currently his main focus. He has been the technical manager of the Italian projects WISE-WAI and

NAUTILUS, and is currently involved in research efforts funded by the European Community and related to underwater acoustic networking. He served in the organizing committee of several conferences, and has been guest editor for the Hindawi Journal of Electronics and Computer Engineering special issue on “Underwater Communications and Networking.” His research interests include many aspects of underwater communications, such as channel modeling, network performance evaluation, cross-layer protocol design and at-sea experiments.



Leonardo Badia in Ferrara, Italy, in 1977. He received the Laurea Degree (with honors) in Electrical Engineering and the PhD in Information Engineering from the University of Ferrara, Italy, in 2000 and 2004, respectively. During 2002 and 2003, he was on leave at the Radio System Technology Labs (now Wireless@KTH), Royal Institute of Technology of Stockholm, Sweden. After having been with the Engineering Department of the University of Ferrara, he joined in 2006 the IMT Institute for Advanced Studies, in Lucca, Italy. In 2011,

he moved to the University of Padova, where he is currently an Assistant Professor.

His research interests include protocol design for multi-hop networks, cross-layer optimization of wireless communication, transmission protocol modeling, and applications of game theory to radio resource management. He authored several scientific papers and was involved in the organization of many scientific conferences in the broad area of networking and wireless communications. He presently serves on the Editorial Board of the IEEE Transactions on Communications, and the Wireless Communications Letters, and is an active reviewer for several periodicals and conferences.



Michele Zorzi received his Laurea and PhD degrees in electrical engineering from the University of Padova in 1990 and 1994, respectively. During the academic year 1992–1993 he was on leave at UCSD, attending graduate courses and doing research on multiple access in mobile radio networks. In 1993 he joined the faculty of the Dipartimento di Elettronica e Informazione, Politecnico di Milano, Italy. After spending three years with the Center for Wireless Communications at UCSD, in 1998 he joined the School of Engineering of the University of Ferrara, Italy, where he became a professor in 2000. Since November 2003 he has been on the faculty of the Information Engineering Department at the University of Padova. His present research interests include performance evaluation in mobile communications systems, random access in mobile radio networks, ad hoc and sensor networks, energy constrained communications protocols, and underwater communications and networking. He was Editor-In-Chief of IEEE Wireless Communications from 2003 to 2005 and Editor-In-Chief of the IEEE Transactions on Communications from 2008 to 2011. He was also guest editor for special issues in IEEE Personal Communications (“Energy Management in Personal Communications Systems”) and IEEE Journal on Selected Areas in Communications (“Multimedia Network Radios” and “Underwater Wireless Communications and Networking”). He served as a Member-at-Large of the Board of Governors of the IEEE Communications Society from 2009 to 2011.

He was Editor-In-Chief of IEEE Wireless Communications from 2003 to 2005 and Editor-In-Chief of the IEEE Transactions on Communications from 2008 to 2011. He was also guest editor for special issues in IEEE Personal Communications (“Energy Management in Personal Communications Systems”) and IEEE Journal on Selected Areas in Communications (“Multimedia Network Radios” and “Underwater Wireless Communications and Networking”). He served as a Member-at-Large of the Board of Governors of the IEEE Communications Society from 2009 to 2011.